Self-Oscillating Membranes with Polymer Interface Synchronized with Chemical Oscillator to Reproduce Lifelike Pulsatile Flow

Marianne Benoit, Denis Bouyer, Philippe Sistat, André Ayral, Didier Cot, Bertrand Rebiere, David Fournier, Joel Lyskawa, Patrice Woisel, Claire Antonelli, et al.

Self-oscillating Membranes with Polymer Interface synchronized with Chemical Oscillator to Reproduce Lifelike Pulsatile Flow

Marianne Benoit[1], Denis Bouyer[1], Philippe Sistat[1], André Ayral[1], Didier Cot[1], Bertrand Rebiere[2], David Fournier[3], Joël Lyskawa[3], Patrice Woisel[3], Claire Antonelli[1]*, and Damien Quemener[1]*

[1] Institut Européen des Membranes, IEM-UMR 5635, Univ Montpellier, ENSCM, CNRS, Montpellier, France. claire.antonelli@umontpellier.fr ; damien.quemener@umontpellier.fr

[2] Institut Charles Gerhardt, UMR5253, CNRS-UM-ENSCM, Univ Montpellier, Montpellier, France

[3] Univ, Lille, CNRS, INRAE, Centrale Lille, UMR 8207 –UMET- Unité Matériaux et Transformations, F-59000 Lille, France

ABSTRACT: Self-oscillating filtration membranes having a lifelike pulsatile flow are prepared thanks to a synchronized coupling between a chemical oscillator and a responsive membrane. Commercial alumina membranes are superficially functionalized with pH-responsive poly(methacrylic acid) (PMAA) chains synthesized by Reversible Addition-Fragmentation chain Transfer (RAFT) polymerization of MAA in the presence of a catechol-based RAFT agent. The grafting of PMAA onto alumina, mediated through catechol chemisorption, is analyzed by X-ray Photoelectron Spectroscopy, Scanning Electron Microscopy combined with Energy Dispersive X-ray spectroscopy and static water contact angle. Bromate-Sulfite-Ferrocyanide (BSF) is used as a chemical oscillator, enabling autonomous cyclic pH-modulation between 3.5 and 6.5. pH oscillations are setup in the conditions of membrane filtration inside a filtration cell thanks to a careful study of the bifurcation diagram giving the required conditions to reach the oscillation domain. Since PMAA has a pKa around 5.8, a periodic extension-contraction of the polymer chains is obtained during membrane filtration which leads to a synchronized change in the membrane pore size. Chemically-powered autonomous pulsatile flow with impressive permeability cycles is observed with an effective chemomechanical feedback action of the membrane pore size change on the chemical oscillator mechanism.

INTRODUCTION

Biological systems have an unique ability to communicate with their local environment through chemical and mechanical energy interconversions.[1] This process is based on a network of chemical reactions that a biological cell, for example, is able to read as a written language in order to make decisions. In general, the understanding of complex biological systems through the prism of the network language represents nowadays a very active interdisciplinary field of research which could drive to the emergence of a new generation of lifelike materials.[2]

Most nowadays synthetic materials are unable to operate autonomously because of their limited communication skills.[3] However structural changes can be triggered by mechanical or chemical signals leading to the expression of a specific function, which is encouraging but not sufficient.[4] So-called "smart" materials have been designed to respond to a variety of stimuli, such as pH,[5] temperature,[6] mechanical strength,[7] biological triggers,[8] and electromagnetic fields.[9] Various applications have been developed with this principle, such as sensors,[10] drug carriers[11] or actuators.[12] However, in these systems, the response of polymer materials is one-way in the sense that only one action is achieved when the stimulus is on. For example, when the temperature is increased over approximately 32°C, poly(N-isopropylacrylamide) chains exhibit dramatic change from an extended random coil to a compact conformation.[13] As a result, a repetitive on/off switching of external stimuli is necessary to cause the two-way action of these materials. The main drawback of stimuli-sensitive materials is therefore their lack of autonomy to produce cyclic structural changes.

In this regard, oscillating reactions with large pH variations have been shown to induce periodic volume changes of a polymer gel immersed in the reacting solution. A. Yoshida reported in 1996 a pioneering work that paved the way for the development of self-oscillating polymer materials.[14] In this study, a copolymer was prepared by random copolymerization of N-isopropylacrylamide (NIPAAm) and a Ru(bpy)3 vinyl derivative. Interestingly, poly(NIPAAm-co-Ru(bpy)$_3$) has a cloud point temperature (T_{cp}) that varies depending on the oxidation state of the transition metal. Belousov-Zhabotinsky (BZ) chemical oscillator, involving the oxidation of an organic acid by bromate ion in the presence of a metal-ion catalyst under acidic conditions, was used. The cyclic permutation of $Ru(bpy)_3^{2+}$ to $Ru(bpy)_3^{3+}$ modulates the hydrophilicity of the copolymer, resulting in a continuous change in T_{cp}.

Table 1. Chemical reactions involved in the BSF mechanism

Index	Reaction
1	$SO_3^{2-} + H^+ \rightleftharpoons HSO_3^-$
2	$HSO_3^- + H^+ \rightleftharpoons H_2SO_3$
3	$3\ HSO_3^- + BrO_3^- \rightarrow 3\ SO_4^{2-} + Br^- + 3\ H^+$
4	$3\ H_2SO_3 + BrO_3^- \rightarrow 3\ SO_4^{2-} + Br^- + 6\ H^+$
5	$BrO_3^- + 6\ Fe(CN)_6^{4-} + 6H^+ \rightarrow Br^- + 6\ Fe(CN)_6^{3-} + 3\ H_2O$
6	$SO_4^{2-} + H^+ \rightleftharpoons HSO_4^-$
7	$H_2SO_4 \rightarrow HSO_4^- + H^+$

Since $Ru(bpy)_3$ acts as a catalyst for the BZ reaction, a gel made from cross-linked poly(NIPAAm-co-$Ru(bpy)_3$) exhibits an autonomous swelling–deswelling oscillation driven by the transition metal redox oscillation. Since this first report, autonomous oscillating polymer materials have been thoroughly studied[15–24] and applications in biomimetic soft actuators,[25–28] functional fluids,[29–34] and mass transport systems[35–39] have been explored.

In this work, self-oscillating hybrid filtration membranes whose flow is made pulsatile in a way similar to blood flow is described. For this, an alumina membrane functionalized by a pH-sensitive polymer is synchronized with a pH oscillator. A network of chemical reactions with a feedback loop will produce pH cycles in the surrounding environment. The polymer material will then "read" the chemical information and translate it into macroscopic structural change. This new coupling allows constant communication between the membrane and its environment and constitutes an essential step towards the synthesis of autonomous lifelike materials.

RESULTS AND DISCUSSION

To prepare the self-oscillating system, the surface of an alumina membrane has been functionalized with a pH-sensitive polymer, the α-dopamine-poly(methacrylic acid) (Dopa-PMAA) (Figure 1a). Since the polymer is present at the interfaces of the membrane, its conformation (globular or extended) - which is linked to the surrounding pH - will directly impact the value of the water flux via a modulation of the pore size.

In order to implement the self-oscillating behavior, the pH-sensitive hybrid membrane is then mounted into a filtration setup and coupled with pH-oscillator system in solution (Bromate-Sulfite-Ferrocyanide, BSF) (Figure 1b). BSF pH oscillator mechanism has been reported by Rábai, Kaminaga and Hanazaki (RKH) (reactions 1-5, Table 1),[40] further extended by Sato et al. by adding the protonation equilibrium of SO_4^{2-} (reaction 6).[41] When the SO_3^{2-} species is present, reactions 1 and 3 predominate and the stoichiometric balance shows a stable and low concentration of H^+. The pH of the oscillator is then at its highest. When the concentration of SO_3^{2-} drops sufficiently due to its consumption, a large quantity of H^+ is produced and the species H_2SO_3 is then generated via reaction 2. The couple of reactions 2 and 4 then lead to an autocatalytic production of H^+ which drops the pH sharply. The reaction 5 acts, for its part, as a negative feedback which consumes H^+ continuously. The behavior of nonlinear systems depends essentially on their control parameters, namely the initial concentrations of each species introduced and the flow of reactants passing through an open reactor. When one is far from the thermodynamic equilibrium of the reactions, the oscillating BSF system can exhibit abrupt cyclical changes of pH in an area defined both by the residence time of the reactants and their concentration called the oscillating domain.

The pH change directly modulates the ionization degree of PMAA chains grafted on alumina membranes. For low values of degree of ionization ($\alpha < 0.2$) (pKa ~ 5.8), PMAA chains adopt a globular conformation and are strongly folded because of "hydrophobic" interactions from methyl groups (Figures S1-S3, Supporting Information). The membrane pores are then in an “open” state (Figure 1c). When deprotonating the PMAA blocks beyond their pKa, the dissociated groups are therefore very close to one another, which leads to an accumulation of electrostatic energy. Above a threshold value of $\alpha = 0.20$, polymer chains can no longer support the accumulation of electrostatic energy and their conformation suddenly change into more stretched chains for which the distance between ionized groups increases (pores in a “close” state).[42] The cyclic change in pore size is synchronized with the pH-oscillation, yielding periodical change of the membrane permeability (Figures S8-S12, Supporting Information).

Dopa-PMAAx of three different molecular weights (X: degree of polymerization = 23, 48, 62, Table S1, Supporting Information) have been prepared by reversible addition-fragmentation chain-transfer (RAFT) polymerization with a dopamine-functionalized RAFT agent in order to elaborate catechol end-functionalized polymers. Commercial alumina membranes were functionalized (Figure 1a) by immersion in a Dopa-PMAA solution (0.044 mol L-1) and left under elliptical stirring at 100 rpm for 16 hours in the absence of light. Membranes were then rinsed by immersion in demineralized water for one hour and then introduced in the filtration cell.

Carboxylic acid groups are known to directly interact with alumina surface so PMAA prepared by RAFT polymerization bearing no dopamine as end-group was tested first.[43] X-ray Photoelectron Spectroscopy (XPS) of the membrane functionalized with PMAA witness its successful deposition (Figures S22 and S27, Supporting Information). However, when used in a filtration setup with pH oscillations, the permeability of the membrane was found to weakly oscillate which is a consequence of a weak change of the PMAA chain conformation at the membrane pore surface (Figure S11, Supporting Information). This could be ascribed to a strong chemisorption through multiple carboxylic acid groups along the polymer chains leading to a low degree of mobility. On the contrary, the presence of a dopamine end-group was found to considerably increase the oscillation amplitude in permeability which seems to be preferentially linked to the membrane through its extremity, giving more freedom to the polymer chain to contract/extend in relation with the pH.

The grafting of the three Dopa-PMAA on the alumina membrane surface has been characterized by XPS, Scanning Electron Microscopy combined with Energy Dispersive X-ray spectroscopy (SEM-EDX) and static contact angle. XPS survey scans of PMAA-grafted alumina surfaces revealed an increase of C1s peaks (285 eV) and decrease in Al2p peaks (74 eV) as compared to the ungrafted sample (Figures S18-S21, Supporting Information). With a XPS analysis thickness of approximately 100 Å, it confirms the successful superficial grafting of the PMAA. Moreover, the relative atomic composition indicates enrichment in PMAA at the surface when the degree of polymerization is increased from 23 to 48 and then to 62 (Table S2, Supporting Information). The grafting is further confirmed in high-resolution C1s scans with the presence of two peaks at 286.3 and 288.7 eV corresponding respectively to C-O and C=O coming from PMAA carboxylic acid groups (Figures S23-S26, Supporting Information). SEM-EDX enabled us to get more insight on the polymer grafting location, i.e. on the external surfaces or/and inside the pores. SEM-EDX color mapping images of Carbon (Figure 2a and Figures S28-S29, Supporting Information) discriminate two groups of polymers. For X=23 and 48, a progressive decrease of PMAA amount inside the membrane pores is observed with a grafting depth of about 1µm. For PMAA62, the EDX color mapping image is similar to that of the ungrafted alumina. Combined with the results observed in XPS, the conclusion is that the two smallest PMAA (X=23, 48) could freely diffuse and be grafted inside the membrane pores whereas the longest with X=62 seems to be excluded by sieving effect and was therefore mostly grafted at the membrane external surface as illustrated in Figure 1b. The grafting reaction did not alter the macroscopic membrane morphology as show SEM images of the surface and cross-section (Figures S30-S32, Supporting Information).

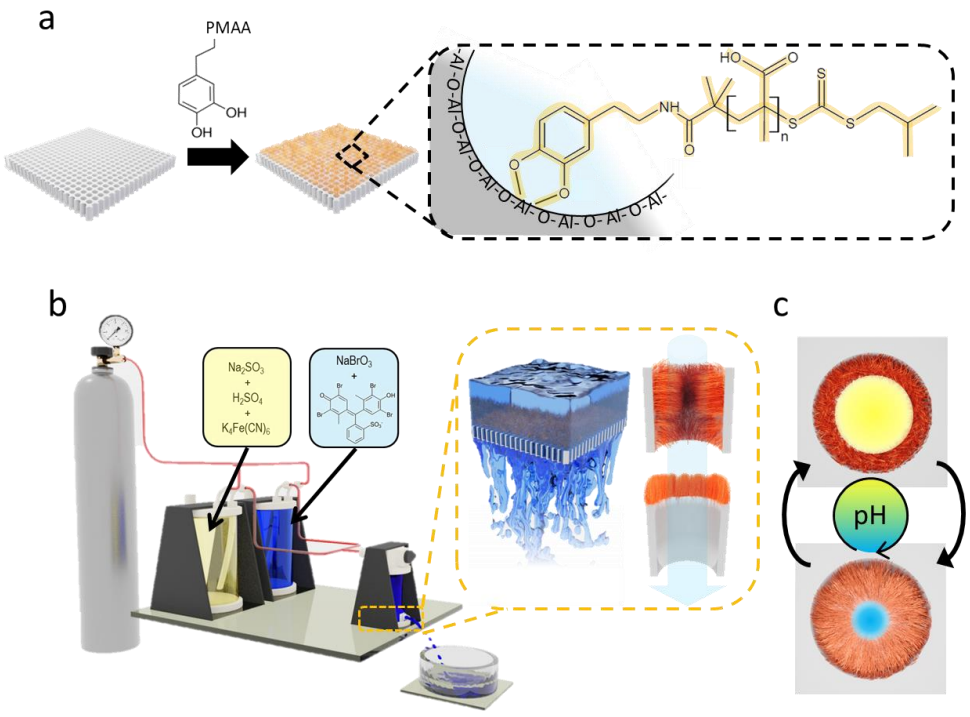

Figure 1. a) Functionalization of an alumina membrane by reaction with poly(methacrylic acid) ended with a catechol. The enlargement shows chemisorption of the polymer chain in a pore. b) Process of filtration with self-oscillating membranes. Two tanks containing sulphite and ferrocyanide on one hand, and bromate on the other, are pressurized and connected to a dead-end filtration cell. Sulfuric acid and a *pH*-indicator (bromocresol green) are added to accelerate and visualize *pH* oscillations, respectively. The enlargement shows the alumina membrane functionalized by poly(methacrylic acid) during filtration (left) and two different functionalization configurations (superficial and in the pore). c) Schematic illustration of pore size control via contraction-extension cycles of polymer chains. Blue and yellow colors refer to neutral and acid *pH*, respectively.

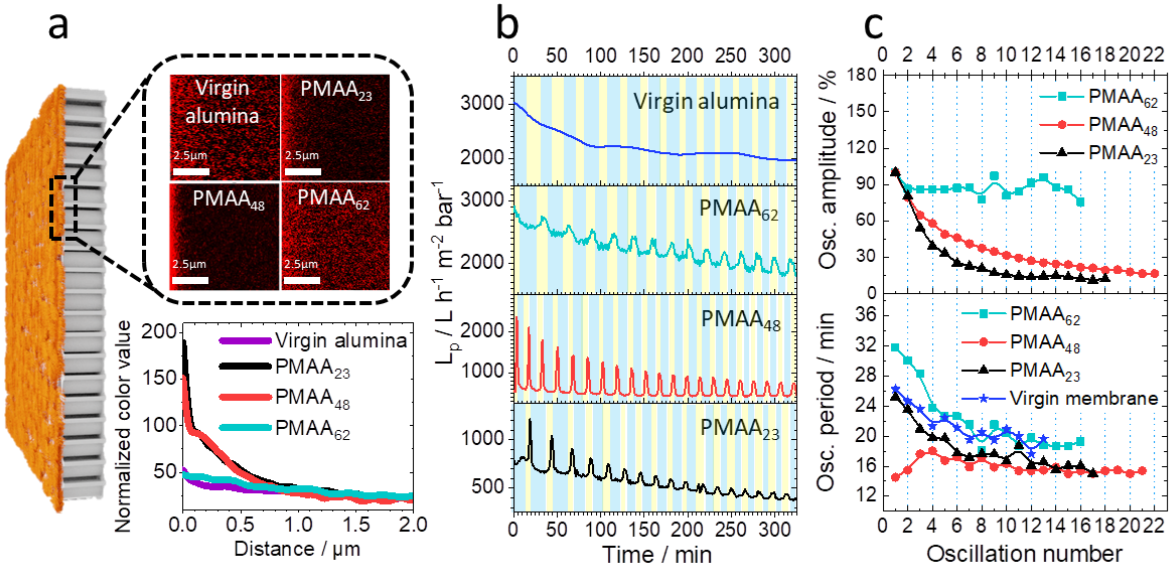

Figure 2. a) Energy Dispersive X-ray spectroscopy mapping of Carbon made on the cross-section of modified alumina membranes and a virgin membrane. Images are going from the top surface to the bottom side from the left to the right. b) Variation in permeability of three alumina membranes modified with dopamine terminated poly(methacrylic acid) with different degrees of polymerization $PMAA_{62}$, $PMAA_{48}$, $PMAA_{23}$ and a virgin membrane. The oscillatory domain was reached by applying a pressure drop of 0.2, 0.2, 0.4 bar for $PMAA_{62}$, $PMAA_{48}$, $PMAA_{23}$, respectively. The striped lines represent the *pH* oscillation periods in the filtration cell: yellow for acid *pH* and blue for neutral *pH*. c) Comparison of the oscillation amplitude and period of the membranes.

The water contact angle increases by 3 to 6° when comparing a drop of acidic water (pH=3.2) to a drop of demineralized water (pH=6.8) (Table S3, Supporting Information) whereas no change was observed with the ungrafted membrane. As explained before, at pH above the pKa of PMAA, the polymer chains adopt an extended conformation with the presence of negatively charged carboxylate ions increasing the surface hydrophilicity. On the contrary, for a pH below the pka, PMAA chains are collapsed with protonated carboxylic groups, which is in agreement with a water contact angle increase. A continuous stirred tank reactor (CSTR) filtration setup, thermally regulated at 30°C, was used for all filtration experiments (Figure 1b). The aqueous feed solutions separated in two tanks enter premixed at the same flow rate into the CSTR (Tank 1: $[KBrO_3]_0$ = 75 mM and [sodium bromocresol green]$_0$= 0.11 mM; Tank 2: $[Na_2SO_3]_0$ = 70 mM, $[K_4Fe(CN)_6]_0$ = 15 mM, $[H_2SO_4]_0$ = 7.5 mM). BSF pH oscillator was set up in the filtration cell under pressure and the relative pH evolution was monitored by video acquisition of the solution color change thanks to a pH indicator (bromocresol) (Figures S10 and S12, Supporting Information). The pH oscillator allows cyclic variations of the pH with wide and regular amplitude of oscillations between 3.5 and 6.5 under the membrane filtration conditions.

Water permeation was carried out with all membranes while targeting the oscillation domain by a modulation of the pressure drop across the membrane which changes the residence time in the filtration cell (Figure 2b). Whereas no cyclic modulation of permeability was observed with the virgin membrane as expected, all membranes were characterized by continuous permeability decrease. This has been reported to be the consequence of the dissolution of water-soluble $[Al_{13}O_4(OH)_{24}(H_2O)_{12}]^{7+}$ polyhydroxocomplexes which then will clog part of the membrane pores after deposition.[44] It can be mentioned that a possible strategy to avoid membrane erosion, and which could be the subject of a perspective in this work, would be to use a protective layer, such as polydopamine, before the functionalization of the membrane by the PMAA.[45] Nevertheless, a chemically-powered autonomous pulsatile flow was clearly observed with the Dopa-PMAA-functionalized membranes thanks to extension-contraction cycles of the polymer chain directly correlated with the fluctuations of pH (Figure S12, Supporting Information). To suppress the permeability decrease effect, oscillation amplitudes were measured (Figure 2c) and compared. Two cases could be differentiated whether oscillation amplitude was stable over time ($PMAA_{62}$) or a dampening that seems to find a certain balance over time was observed ($PMAA_{23}$ and $PMAA_{48}$). A correlation could be made with the grafting location since $PMMA_{62}$ was mostly found on the very top surface whereas the shorter polymers were also grafted at membrane pore walls. In confined environment of a pore, it is proposed that successive extension-contraction of polymer chains could lead to a reorganization of interactions in between polymer chains as well as between polymer chains and pore walls. An increase of the interaction number would decrease the oscillation amplitude until a new equilibrium is reached. Without any confinement effect, membrane with $PMAA_{62}$ seems to undergo fully reversible extension-contraction cycles without questioning the nature and

number of interactions. In fact, for this polymer, the amplitude of the oscillations is constant as shown in Figure 2c ($PMAA_{62}$) which indicates that the "closed" and "open" pore configurations are stable over time and therefore that the cycles extension-contraction of PMAA chains are reversible.

The evolution of the oscillation period is more difficult to understand since it is directly related to the interplay between the membrane and the pH oscillator (Figure 2c).

In order to get more insight about the effect of coupling the pH-oscillator to a pH-responsive membrane, one parameter bifurcation diagram was elaborated. The behavior of non-linear systems crucially depends on their control parameters such as the initial concentrations of each introduced species. When the reaction is constrained to stay far from thermodynamic equilibrium, non-linear systems exhibit sudden changes in behavior, referred as bifurcation. By drawing a bifurcation diagram in the vicinity of this one, it is then possible to define a concentration domain making possible to observe oscillations.

BSF oscillations were thus carried out with an ungrafted membrane and the normalized flow rate (reverse of residence time) k_o was varied in the range of $1\times10^{-4}\ s^{-1} < k_o < 5\times10^{-3}\ s^{-1}$ thanks to a modulation of the membrane pressure drop (Figure 3a and Figures S4-S7, Supporting Information). An oscillation domain was observed between $4.5\times10^{-4}\ s^{-1}$ and $1.7\times10^{-3}\ s^{-1}$, surrounded by two steady states at "low" pH (SSL) and "high" pH (SSH) (Figure 3b). Interestingly, when a Dopa-PMAA-functionalized membrane is used instead, oscillations outside the previously established oscillatory domain were observed (Figure 3a,c). This, coupled with the evolution of the oscillation periods in Figure 2c, is a clear sign that the pH-responsive membrane is directly interplaying in the pH-oscillator mechanism. Without any feedback loop of the membrane on the pH-oscillator, a "low" pH would have opened the membrane pores giving an increased flux whereas a "high" pH would have partially closed the membrane pores yielding to a flux decrease (Figure 3d). However, the flux value directly impacts the residence time in the filtration cell and thus the k_o. When the pH is "low" (L-Osc), PMAA chains are collapsing on the pore walls, pores are thus opening, thereby k_o is increasing and could exit from the oscillation domain to reach SSH branch which would increase the pH (Figure 3e). At such "high" pH, PMAA chains are extending inside the pores thus closing them; k_o is then decreasing which brings back the system into the oscillation domain. The dynamic interplay between autonomous pH changes and multiscale motions is the key element in many living organisms.[46]

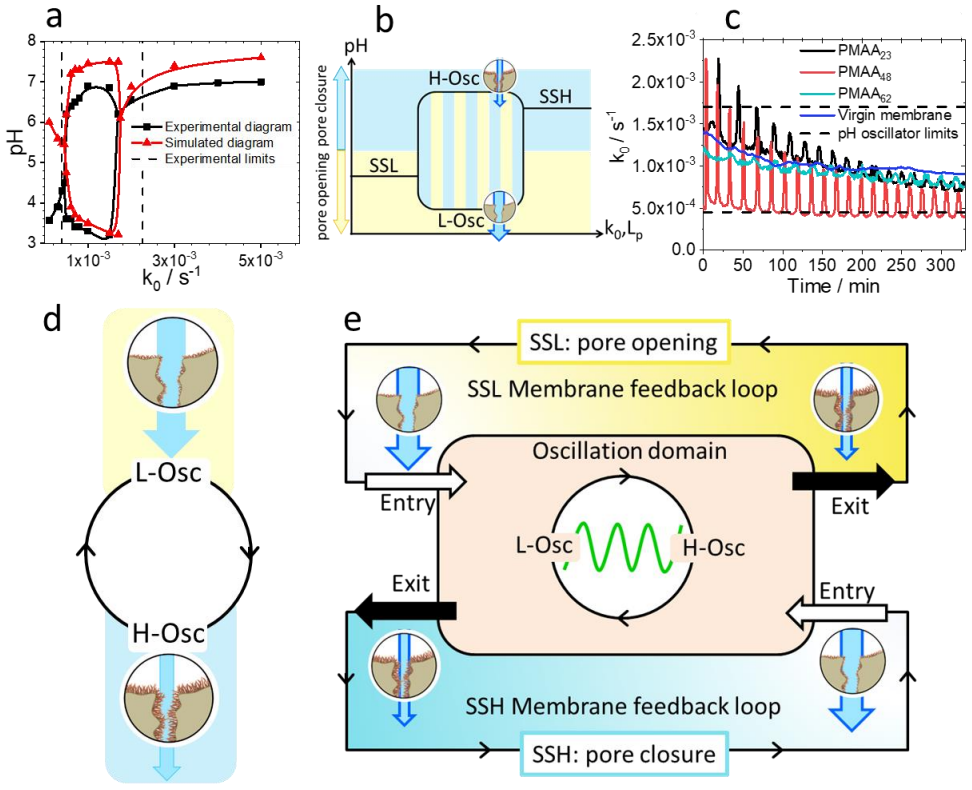

Figure 3. a) One-parameter bifurcation diagrams. The black curve is the experimental bifurcation diagram as measured by stepwise variation of k_o while the red curve is the simulated bifurcation diagram. The two dashed lines correspond to the experimental k_o area of *pH* oscillations observed in the presence of a PMAA-functionalized membrane. b) Schematic illustration of a bifurcation diagram. SSL: Steady State at "Low" *pH*, SSH: Steady State at "High" *pH*, H-Osc: "High" *pH* branch of the oscillation domain, L-Osc: "Low" *pH* branch of the oscillation domain. c) Variation of flow rate k_o of modified membranes $PMAA_{23}$, $PMAA_{48}$, $PMAA_{62}$ and the virgin membrane against filtration time. d) Simplified mechanism of coupling between *pH* oscillation and membrane pore size change. e) Proposed feedback action of mechanical pore size change onto the *pH*-oscillator.

Here the chemomechanical feeback loop makes the self-oscillation system working only because the mechanical effect of the pore size change on the flux -and indirectly on the pH- enables to exit and come back inside the oscillation domain. By modeling the BSF pH oscillator (see Part 3.9, Supporting Information), the theoretical bifurcation diagram was drawn and found to be in agreement with the experimental one in terms of oscillating domain (Figure 3a). Simulations were then performed in order to understand why flux oscillations can be observed outside the pH oscillation domain. When a simulation run is launched with a variable k_o based on experimental data ($PMAA_{48}$), which oscillates depending on the pore opening, the pH oscillates too, following the same trend as k_o oscillations (Figure S35, Supporting Information). Experimental k_o oscillates from maxima and minima that depend on time going from 3.8×10^{-4} s^{-1} to 2.2×10^{-3} s^{-1}. However, when a constant k_o of 1.8×10^{-3} s^{-1} is imposed, the simulated oscillations rapidly stopped, leading to constant pH value around 6.5 (SSH branch) (Figure S34, Supporting Information). But, when looking back at the variation of pH for oscillating k_o, the two first maxima reached by the system exceed this value of 1.8×10^{-3} s^{-1} and the system was shown to keep on oscillating, while a rapid oscillation damping would have been expected. The comparison between those two simulations exhibit that the oscillations were maintained thanks to the membrane action, which brings the system back from SSH within the oscillating region of the bifurcation diagram. The same conclusion can be drawn when launching a simulation considering a low constant k_o of 4.4×10^{-4} s^{-1} (Figure S33, Supporting Information). A progressive oscillation damping can be observed in the simulation since the system is slightly out of the bifurcation region. However, experimental k_o values lower than 4.4×10^{-4} s^{-1} were reached and the oscillation were shown to be maintained. In this case too, the oscillations continue because the membrane brings back the system from SSL branch into the bifurcation region. The role of the membrane in the oscillation dynamics is clearly demonstrated by comparing experimental and simulated data.

CONCLUSIONS

In conclusion, dopamine end-functionalized pH-sensitive polymers have been successfully prepared by RAFT polymerization and grafted onto alumina membrane. The grafting of PMAA was characterized and confirmed by XPS, SEM-EDX and contact angle investigations. BSF oscillator was set up in filtration cell and showed a periodic and autonomous change of the pH between 3.5 and 6.5. Coupled with the pH-responsive membrane, it induced an impressive autonomous periodic change in permeability due to extension-contraction cycles of PMAA chains. The chemically-powered autonomous pulsatile flow has turned a commercial filtration membranes into a lifelike materials characterized by an effective chemomechanical feedback loop. A higher degree of autonomy could be reached by integrating the oscillator components into the membrane structure and it will constitute the perspectives of this work. These bio-inspired filtration membranes able to communicate and respond autonomously to their environment represent a step forward in a new exciting field of study on lifelike materials.

EXPERIMENTAL SECTION

Chemicals. All chemicals and solvents were obtained from commercial sources and used as such unless otherwise noted. Methacrylic acid (99%, Sigma Aldrich) was purified over inhibitor remover column prior to use. 4,4'Azobis(4-cyanovaleric acid) (ACVA) (≥98%), Trioxane (≥99%), 4-Cyano-4-(phenylcarbonothioylthio)pentanoic acid were purchased from Sigma-Aldrich. Ethanol absolute (100%), methanol (hypersolv chromanorm, 100%) were purchased from VWR and Toluene (99.8%) from Fisher Scientific. The Dopa-CTA RAFT agent was synthesized as previously described.[47] All polymerizations were conducted in a nitrogen atmosphere. Reagent grade Potassium hexacyanoferrate (II) trihydrate (98+%, Alfa Aesar), Sodium sulfite (≥98%, Bioultra, anhydrous), sulfuric acid (Sigma Aldrich, 95-97%) and Bromocresol green (Sigma-Aldrich) were used without further purification. Solutions were prepared one hour before each run in demineralized water. Alumina Anodisc™ membranes filters (Whatman Inc., UK) were used. Its nominal pore size is 0.02µm with 25mm of diameter. The filters are flat disks of alumina manufactured by controlled anodization of aluminium sheets. They exhibit an asymmetric structure consisting of a thin surface layer (~ 1µm) with a pore size of ~ 0.02 µm and a thicker support layer (~ 60 µm) with a pore size of ~ 0.2 µm.

Characterization. ^{1}H NMR spectra were recorded at room temperature on Bruker Avance spectrometers operating either at 400 or 600 MHz using deuterated DMSO. Size Exclusion Chromatography was carried out on a Viscotek device (Malvern instruments, Worcestershire, UK) having triple detector array. The Viscotek SEC apparatus was equipped with two OHpak SB-806M HQ columns using $NaNO_3$ (0.2 mol L^{-1}) aqueous solution as an eluent with flow rate of 0.7 mL min^{-1} at 35°C. Membrane cross section, top surface and bottom surface were analyzed by Scanning Electron Microscopy (SEM). The SEM pictures were obtained using a Hitachi S4800 operating under 0.1-30kv working voltage. Energy-dispersive X-ray spectroscopy analysis (EDX) was taken with Zeiss EVO HD15 microscope coupled with an Oxford X-MaxNSDD EDX detector. The wetting characteristics of all membranes were determined using a contact angle goniometer (Digidrop gbx) via static demineralized water contact angle measurements with water drops of size ~ 30 µl using the Laplace–Young method. The water contact angle (WCA) measurements are an average of three measurements repeated on the same membrane. It has to be mentioned that a kinetic effect (WCA decreasing with time) was observed at acid pH for $PMAA_{23}$ and $PMAA_{48}$ functionalized membranes. The presence of hydrophilic polymer chains in the membrane pores for $PMAA_{23}$ and $PMAA_{48}$ could facilitate the water intrusion into the membrane thus explaining the water contact angle decrease. The permeability of membrane discs (diameter = 2.5 cm) was estimated by filtration test. The membranes were fitted in a 10 mL filtration cell (Amicon 8010 stirred

cell) connected to a water reservoir and a compressed air line. The measurements were then performed at pressures between 0 and 1 bar. The mass of water passing through the membrane (permeate) was recorded using a connected balance at regular time intervals. All filtration experiments were performed at 30°C (solutions were pre-heated in Stuart SW6 series bath) with demineralized water. X-Ray photoelectron spectrometry (XPS) was carried out with the ESCALAB 250 device from ThermoElectron. The excitation source was the monochromatic source, Al Kα line (1486.6 eV). The surface analyzed has a diameter of 500 µm. Photoelectron spectra were calibrated in binding energy with respect to the energy of the C-C component of carbon C1s at 284.8 eV.

Synthesis of PMAA from Dopa-CTA. A representative example for MAA polymerization in ethanol is as follows: in a round bottom flask Dopa-CTA (55 mg, 0.14 mmol), ACVA (4 mg, 0.014 mmol), Trioxane (0.18 g, 2 mmol) were dissolved in MAA (1g, 11.5 mmol) and 4.8 mL of EtOH. Trioxane was used as an internal reference for NMR. The resulting mixture was deoxygenated by nitrogen bubbling for 30 min and immersed in an oil bath thermostated at 70°C during 8h30. The monomer conversion was determined by ^{1}H NMR spectroscopy in DMSO-d^6 by the relative integration of the protons of 1,3,5-trioxane and the vinylic protons of MAA. ^{1}H NMR (600MHz, DMSO-d^6, δ (ppm)): 12.31 (s, broad, 1H, COOH of PMAA); 8.73 (s, H, Aryl-OH); 8.60 (s, H, Aryl-OH); 7.83 (m, J = 8 Hz, 2H, o-2H-Ph of chain end CTA); 7.62 (m, J = 8 Hz, 1H, p-H-Ph of chain end CTA); 7.5 (s, NH-CH_2-CH_2); 7.46 (m, J = 7 Hz, 2H, m-2HPh of chain end CTA); 2.39 (m, 4H, CH_2CH_2 of chain end from CTA); 2-0.91 (m, 5H, methylene and methyl protons of PMAA).

Synthesis of PMAA from 4-Cyanopentanoic acid dithiobenzoate (CADB) as RAFT agent. A representative example for MAA polymerization in ethanol is as follows: in a round bottom flask CADB (80 mg, 0.29 mmol), ACVA (8mg, 0.029 mmol), Trioxane (0.18 g, 2 mmol) were dissolved in MAA (2 g, 22.9 mmol) and 4.8 mL of EtOH. Trioxane was used as an internal reference for NMR. The resulting mixture was deoxygenated by nitrogen bubbling for 30 min and immersed in an oil bath thermostated at 70°C during 8h30. The monomer conversion was determined by ^{1}H NMR spectroscopy in DMSO-d^6 by the relative integration of the protons of 1,3,5-trioxane and the vinylic protons of MAA. ^{1}H NMR (400 MHz, DMSO-d^6, δ): 12.33 (s, broad, 1H, COOH of PMAA); 7.83 (m, J=8Hz, 2H, o-2H-Ph of chain end CTA); 7.62 (m, J=8Hz, 1H, p-H-Ph of chain end CTA); 7.46 (m, J = 7 Hz, 2H, m-2HPh of chain end CTA); 2.35 ppm (m, 4H, CH_2CH_2 of chain end from CTA); 2-0.93 ppm (m, 5H, methylene and methyl protons of PMAA).

ASSOCIATED CONTENT

Supporting Information. Structural characteristics of PMAA; X-Ray Photoelectron Spectroscopy results; Water contact angle at acid and neutral pH; Potentiometric titration of PMAA; Construction of one-parameter experimental bifurcation diagrams; Permeability; Nuclear Magnetic Resonance (NMR); Size Exclusion Chromatography (SEC); X-ray Photoelectron Spectroscopy (XPS); Energy Dispersive X-ray spectroscopy (EDX); Scanning Electron Microscopy (SEM); Modeling. This material is available free of charge via the Internet at http://pubs.acs.org.

AUTHOR INFORMATION

Corresponding Authors

Damien Quemener - Institut Européen des Membranes, IEM-UMR 5635, Univ Montpellier, ENSCM, CNRS, Montpellier, France. damien.quemener@umontpellier.fr
Claire Antonelli - Institut Européen des Membranes, IEM-UMR 5635, Univ Montpellier, ENSCM, CNRS, Montpellier, France. claire.antonelli@umontpellier.fr

Author Contributions

D.Q. designed and managed the project together with C.A. M.B. carried out the synthesis and characterizations of polymers and membranes. D.B. and P.S. carried out the data simulation. A.A. analyzed the results of filtration with the alumina membranes. D.C. and B.R. performed the SEM and EDX. D.F., J.L. and P.W. synthesized the Dopa-RAFT agent and discussed the results in SEC. D.Q. and M.B. wrote the initial manuscript. All authors contributed to the writing of the manuscript.

Notes

The authors declare no conflict of interest.

ACKNOWLEDGMENT

Valérie Flaud, Felix Krusch, and Mohamed Hanafi are acknowledged for XPS, PMAA titration, and SEC respectively. D.Q. acknowledges financial support from Institut Universitaire de France (IUF). D.F., J.L. and P.W. acknowledge the project ARCHI-CM, Chevreul Institute (FR 2638), Ministère de l'Enseignement Supérieur et de la Recherche, Région Nord-Pas de Calais and European Regional Development Fund (FEDER) for supporting and funding this work.

REFERENCES

(1) Yashin, V. V.; Kuksenok, O.; Dayal, P.; Balazs, A. C. Mechano-Chemical Oscillations and Waves in Reactive Gels. *Rep. Prog. Phys.* **2012**, *75* (6), 066601. https://doi.org/10.1088/0034-4885/75/6/066601.

(2) Gosak, M.; Markovič, R.; Dolenšek, J.; Slak Rupnik, M.; Marhl, M.; Stožer, A.; Perc, M. Network Science of Biological Systems at Different Scales: A Review. *Physics of Life Reviews* **2018**, *24*, 118–135. https://doi.org/10.1016/j.plrev.2017.11.003.

(3) Walther, A. Viewpoint: From Responsive to Adaptive and Interactive Materials and Materials Systems: A Roadmap. *Advanced Materials* **2020**, *32* (20), 1905111. https://doi.org/10.1002/adma.201905111.

(4) Wei, M.; Gao, Y.; Li, X.; Serpe, M. J. Stimuli-Responsive Polymers and Their Applications. *Polym. Chem.* **2016**, *8* (1), 127–143. https://doi.org/10.1039/C6PY01585A.

(5) Dai, S.; Ravi, P.; Chiu Tam, K. PH-Responsive Polymers : Synthesis, Properties and Applications. *Soft Matter* **2008**, *4* (3), 435–449. https://doi.org/10.1039/B714741D.

(6) Roy, D.; A. Brooks, W. L.; S. Sumerlin, B. New Directions in Thermoresponsive Polymers. *Chemical Society Reviews* **2013**, *42* (17), 7214–7243. https://doi.org/10.1039/C3CS35499G.

(7) Davis, D. A.; Hamilton, A.; Yang, J.; Cremar, L. D.; Van Gough, D.; Potisek, S. L.; Ong, M. T.; Braun, P. V.; Martínez, T. J.;

White, S. R.; Moore, J. S.; Sottos, N. R. Force-Induced Activation of Covalent Bonds in Mechanoresponsive Polymeric Materials. *Nature* **2009**, *459* (7243), 68–72. https://doi.org/10.1038/nature07970.

(8) Colson, Y. L.; Grinstaff, M. W. Biologically Responsive Polymeric Nanoparticles for Drug Delivery. *Advanced Materials* **2012**, *24* (28), 3878–3886. https://doi.org/10.1002/adma.201200420.

(9) Fernández-Nieves, A. Engineering Colloids with Optical and Geometrical Anisotropies: De-Coupling Size Monodispersity and Particle Properties. *Soft Matter* **2006**, *2* (2), 105–108. https://doi.org/10.1039/B512441G.

(10) Hu, J.; Liu, S. Responsive Polymers for Detection and Sensing Applications: Current Status and Future Developments. *Macromolecules* **2010**, *43* (20), 8315–8330. https://doi.org/10.1021/ma1005815.

(11) Bajpai, A. K.; Shukla, S. K.; Bhanu, S.; Kankane, S. Responsive Polymers in Controlled Drug Delivery. *Progress in Polymer Science* **2008**, *33* (11), 1088–1118. https://doi.org/10.1016/j.progpolymsci.2008.07.005.

(12) Ma, M.; Guo, L.; Anderson, D. G.; Langer, R. Bio-Inspired Polymer Composite Actuator and Generator Driven by Water Gradients. *Science* **2013**, *339* (6116), 186–189. https://doi.org/10.1126/science.1230262.

(13) Fell, H.; Han, Y.; Feijen, J.; Kim, S. W. Effect of Comonomer Hydrophilicity and Ionization on the Lower Critical Solution Temperature of IV-Isopropylacrylamide. *Macromolecules* **1993**, *26* (10), 2496–2500.

(14) Yoshida, R.; Takahashi, T.; Yamaguchi, T.; Ichijo, H. Self-Oscillating Gel. *J. Am. Chem. Soc.* **1996**, *118* (21), 5134–5135. https://doi.org/10.1021/ja9602511.

(15) Yoshida, R.; Sakai, T.; Hara, Y.; Maeda, S.; Hashimoto, S.; Suzuki, D.; Murase, Y. Self-Oscillating Gel as Novel Biomimetic Materials. *Journal of Controlled Release* **2009**, *140* (3), 186–193. https://doi.org/10.1016/j.jconrel.2009.04.029.

(16) Yoshida, R. Self-Oscillating Gels Driven by the Belousov–Zhabotinsky Reaction as Novel Smart Materials. *Advanced Materials* **2010**, *22* (31), 3463–3483. https://doi.org/10.1002/adma.200904075.

(17) Ueki, T.; Yoshida, R. Recent Aspects of Self-Oscillating Polymeric Materials: Designing Self-Oscillating Polymers Coupled with Supramolecular Chemistry and Ionic Liquid Science. *Physical Chemistry Chemical Physics* **2014**, *16* (22), 10388–10397. https://doi.org/10.1039/C4CP00980K.

(18) Tamate, R.; Akimoto, A. M.; Yoshida, R. Recent Advances in Self-Oscillating Polymer Material Systems. *The Chemical Record* **2016**, *16* (4), 1852–1867. https://doi.org/10.1002/tcr.201600009.

(19) Yoshida, R.; Ueki, T. Evolution of Self-Oscillating Polymer Gels as Autonomous Polymer Systems. *NPG Asia Materials* **2014**, *6* (6), e107–e107. https://doi.org/10.1038/am.2014.32.

(20) Soo Kim, Y.; Tamate, R.; Mizutani Akimoto, A.; Yoshida, R. Recent Developments in Self-Oscillating Polymeric Systems as Smart Materials: From Polymers to Bulk Hydrogels. *Materials Horizons* **2017**, *4* (1), 38–54. https://doi.org/10.1039/C6MH00435K.

(21) Masuda, T.; Akimoto, A. M.; Nagase, K.; Okano, T.; Yoshida, R. Artificial Cilia as Autonomous Nanoactuators: Design of a Gradient Self-Oscillating Polymer Brush with Controlled Unidirectional Motion. *Science Advances* **2016**, *2* (8), e1600902. https://doi.org/10.1126/sciadv.1600902.

(22) Homma, K.; Masuda, T.; Akimoto, A. M.; Nagase, K.; Itoga, K.; Okano, T.; Yoshida, R. Fabrication of Micropatterned Self-Oscillating Polymer Brush for Direction Control of Chemical Waves. *Small* **2017**, *13* (21), 1700041. https://doi.org/10.1002/smll.201700041.

(23) Masuda, T.; Akimoto, A. M.; Furusawa, M.; Tamate, R.; Nagase, K.; Okano, T.; Yoshida, R. Aspects of the Belousov–Zhabotinsky Reaction inside a Self-Oscillating Polymer Brush. *Langmuir* **2018**, *34* (4), 1673–1680. https://doi.org/10.1021/acs.langmuir.7b03929.

(24) Merindol, R.; Walther, A. Materials Learning from Life: Concepts for Active, Adaptive and Autonomous Molecular Systems. *Chemical Society Reviews* **2017**, *46* (18), 5588–5619. https://doi.org/10.1039/C6CS00738D.

(25) Tabata, O.; Hirasawa, H.; Aoki, S.; Yoshida, R.; Kokufuta, E. Ciliary Motion Actuator Using Self-Oscillating Gel. *Sensors and Actuators A: Physical* **2002**, *95* (2), 234–238. https://doi.org/10.1016/S0924-4247(01)00731-2.

(26) Maeda, S.; Hara, Y.; Sakai, T.; Yoshida, R.; Hashimoto, S. Self-Walking Gel. *Advanced Materials* **2007**, *19* (21), 3480–3484. https://doi.org/10.1002/adma.200700625.

(27) Shiraki, Y.; Yoshida, R. Autonomous Intestine-Like Motion of Tubular Self-Oscillating Gel. *Angewandte Chemie International Edition* **2012**, *51* (25), 6112–6116. https://doi.org/10.1002/anie.201202028.

(28) Shiraki, Y.; Akimoto, A. M.; Miyata, T.; Yoshida, R. Autonomous Pulsatile Flow by Peristaltic Motion of Tubular Self-Oscillating Gels. *Chem. Mater.* **2014**, *26* (19), 5441–5443. https://doi.org/10.1021/cm503040u.

(29) Sakai, T.; Yoshida, R. Self-Oscillating Nanogel Particles. *Langmuir* **2004**, *20* (4), 1036–1038. https://doi.org/10.1021/la035833s.

(30) Taniguchi, H.; Suzuki, D.; Yoshida, R. Characterization of Autonomously Oscillating Viscosity Induced by Swelling/Deswelling Oscillation of the Microgels. *J. Phys. Chem. B* **2010**, *114* (7), 2405–2410. https://doi.org/10.1021/jp911779j.

(31) Suzuki, D.; Taniguchi, H.; Yoshida, R. Autonomously Oscillating Viscosity in Microgel Dispersions. *J. Am. Chem. Soc.* **2009**, *131* (34), 12058–12059. https://doi.org/10.1021/ja904677g.

(32) Ueki, T.; Takasaki, Y.; Bundo, K.; Ueno, T.; Sakai, T.; Akagi, Y.; Yoshida, R. Autonomous Viscosity Oscillation via Metallo-Supramolecular Terpyridine Chemistry of Branched Poly(Ethylene Glycol) Driven by the Belousov–Zhabotinsky Reaction. *Soft Matter* **2014**, *10* (9), 1349–1355. https://doi.org/10.1039/C3SM51537K.

(33) Ueki, T.; Shibayama, M.; Yoshida, R. Self-Oscillating Micelles. *Chem. Commun.* **2013**, *49* (62), 6947–6949. https://doi.org/10.1039/C3CC38432B.

(34) Ueno, T.; Bundo, K.; Akagi, Y.; Sakai, T.; Yoshida, R. Autonomous Viscosity Oscillation by Reversible Complex Formation of Terpyridine-Terminated Poly(Ethylene Glycol) in the BZ Reaction. *Soft Matter* **2010**, *6* (24), 6072–6074. https://doi.org/10.1039/C0SM00788A.

(35) Yoshida, R.; Murase, Y. Self-Oscillating Surface of Gel for Autonomous Mass Transport. *Colloids and Surfaces B: Biointerfaces* **2012**, *99*, 60–66. https://doi.org/10.1016/j.colsurfb.2011.09.036.

(36) Murase, Y.; Maeda, S.; Hashimoto, S.; Yoshida, R. Design of a Mass Transport Surface Utilizing Peristaltic Motion of a Self-Oscillating Gel. *Langmuir* **2009**, *25* (1), 483–489. https://doi.org/10.1021/la802900б.

(37) Masuda, T.; Hidaka, M.; Murase, Y.; Akimoto, A. M.; Nagase, K.; Okano, T.; Yoshida, R. Self-Oscillating Polymer Brushes. *Angewandte Chemie International Edition* **2013**, *52* (29), 7468–7471. https://doi.org/10.1002/anie.201301988.

(38) Murase, Y.; Hidaka, M.; Yoshida, R. Self-Driven Gel Conveyer: Autonomous Transportation by Peristaltic Motion of Self-Oscillating Gel. *Sensors and Actuators B: Chemical* **2010**, *149* (1), 272–283. https://doi.org/10.1016/j.snb.2010.06.017.

(39) Mao, Z.; Kuroki, M.; Otsuka, Y.; Maeda, S. Contraction Waves in Self-Oscillating Polymer Gels. *Extreme Mechanics Letters* **2020**, *39*, 100830. https://doi.org/10.1016/j.eml.2020.100830.

(40) Rábai, G.; Kaminaga, A.; Hanazaki, I. Mechanism of the Oscillatory Bromate Oxidation of Sulfite and Ferrocyanide in a

CSTR. *J. Phys. Chem.* **1996**, *100* (40), 16441–16442. https://doi.org/10.1021/jp960670k.

(41) Sato, N.; Hasegawa, H. H.; Kimura, R.; Mori, Y.; Okazaki, N. Analysis of the Bromate–Sulfite–Ferrocyanide PH Oscillator Using the Particle Filter: Toward the Automated Modeling of Complex Chemical Systems. *J. Phys. Chem. A* **2010**, *114* (37), 10090–10096. https://doi.org/10.1021/jp106700f.

(42) Robin, C. Structure et Rhéologie Du Poly(Acide Méthacrylique) En Régime Semi-Dilué : Organisation Sous Cisaillement et En Température. These de doctorat, Paris Est, 2016.

(43) Kasprzyk-Hordern, B. Chemistry of Alumina, Reactions in Aqueous Solution and Its Application in Water Treatment. *Advances in Colloid and Interface Science* **2004**, *110* (1), 19–48. https://doi.org/10.1016/j.cis.2004.02.002.

(44) Petukhov, D. I.; Buldakov, D. A.; Tishkin, A. A.; Lukashin, A. V.; Eliseev, A. A. Liquid Permeation and Chemical Stability of Anodic Alumina Membranes. *Beilstein J. Nanotechnol.* **2017**, *8* (1), 561–570. https://doi.org/10.3762/bjnano.8.60.

(45) Capozzi, L. C.; Mehmood, F. M.; Giagnorio, M.; Tiraferri, A.; Cerruti, M.; Sangermano, M. Ultrafiltration Membranes Functionalized with Polydopamine with Enhanced Contaminant Removal by Adsorption. *Macromolecular Materials and Engineering* **2017**, *302* (5), 1600481. https://doi.org/10.1002/mame.201600481.

(46) Grinthal, A.; Aizenberg, J. Adaptive All the Way down: Building Responsive Materials from Hierarchies of Chemomechanical Feedback. *Chemical Society Reviews* **2013**, *42* (17), 7072–7085. https://doi.org/10.1039/C3CS60045A.

(47) Zobrist, C.; Sobocinski, J.; Lyskawa, J.; Fournier, D.; Miri, V.; Traisnel, M.; Jimenez, M.; Woisel, P. Functionalization of Titanium Surfaces with Polymer Brushes Prepared from a Biomimetic RAFT Agent. *Macromolecules* **2011**, *44* (15), 5883–5892. https://doi.org/10.1021/ma200853w.

Table of Contents